17th World Conference on Earthquake Engineering, 17WCEE
Sendai, Japan - September 13th to 18th 2020

INELASTIC TORSIONAL BUCKLING ANALYSIS OF A SINGLE-STORY CUBIC FRAME

I. Fukuda [(1)], K. Ikago [(2)]

[(1)] *Graduate Student, Graduate School of Engineering, Tohoku University, iori.fukuda.q3@dc.tohoku.ac.jp*
[(2)] *Professor, International Research Institute of Disaster Science, Tohoku University, Dr. Eng., ikago@irides.tohoku.ac.jp*

Abstract

This study aims to reveal the occurrence conditions of inelastic torsional buckling in a high-rise steel moment resisting frame (SMRF) considering non-negative post-yielding stiffness. In a previous research, we employed a simple symmetric cubic frame to represent a reduced form of a high-rise SMRF; we performed load-control analysis to elucidate that inelastic global torsional buckling could occur even in a symmetric and concentric SMRF subjected to horizontal forces when yield hinges occur at the beam ends of both the longitudinal and transverse frames in the lower part of the structure because of diagonal loading. In this study, we perform displacement-control analysis to discuss the uniqueness of the rate solution and identify the sufficient condition for bifurcation to occur using the concept of the comparison solid proposed by Hill; an investigation on the consistency of post-bifurcation solutions then follows.

Keywords: P-Delta effect; inelastic buckling; moment-resisting frame; comparison solid; bifurcation

1. Introduction

The risk of low-frequency structures subjected to low-frequency ground motions became known to the public after a devastating fire at the petrochemical complex in Tomakomai caused by sloshing in the 2003 Tokachi-oki Earthquake.

Tsurugi *et al*. [1] simulated the ground motion in Osaka area, whose hypocentral region is Nankai and Tonankai Trough, using a hybrid method with the empirical green function method and 3D finite difference method. They noted that the predominant period and duration increased than expected because of the surface wave caused by a sedimentary basin; thus, they indicated a possibility that the peak ground velocity (PGV) could exceed design level PGV and reach 0.7 m/s. In the 2011 Great East Japan Earthquake, even though the distance from the epicenter was about 800 km, a high-rise building in Osaka suffered a maximum half amplitude of 1.36 m at the top floor [2]. In the northwest region of North America, it is well known that large-magnitude earthquakes have occurred many times around the Cascadia subduction zone (CSZ) [3, 4]; these events are expected to have an average return period of around 500 years. It is considered that the most recent large-magnitude earthquake on the CSZ occurred in 1700; therefore, Petersen *et al*. [5] estimated a 10%–14% possibility that an M9 earthquake will occur along the CSZ within the next 50 years. As shown, it is urgently necessary to evaluate the hazard and risk of large-amplitude and long-duration ground motion.

Many of the 14-story steel buildings in Mexico City, 300 km away from the epicenter selectively resonated and thereby suffered damages in the 1985 Mexico Earthquake because of low-frequency ground motion induced by soft surface soil reclaimed from a lake. The collapse of a 21-storied high-rise building, the Pino Suarez complex, attracted the attention of many researchers [6]. To understand critical behavior like the collapse of a high-rise building during the earthquake mentioned above, we have to take into account the gravity effect, *i.e.* geometrical nonlinearity, which is often ignored in seismic response analysis in structural design practice. Uetani and Tagawa [7] conducted a numerical simulation in which two control models with and without the P-Delta effect were employed. The model that took the P-Delta effect into account exhibited bow-shaped deformation concentration in the lower part when yield hinges were formed in all the beam ends of the lower stories after subjection to the El Centro 1940 NS record whose PGV was normalized to 1.5 m/s. This phenomenon is referred to as the deformation concentration in the lower stories (DCILS) by Uetani and

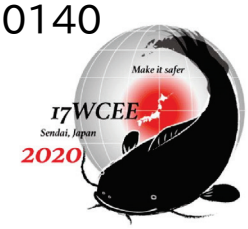

Tagawa [7]. In the last couple of decades, many studies aiming at elucidating the mechanism and proposing countermeasures have been conducted.

DCILS can be observed analytically in a planar frame. Another type of deformation concentration phenomenon was recently found in a numerical simulation analysis of a three-dimensional frame in which geometrical and material nonlinearity were combined. Fig.1 shows the snapshot of the time history response analysis in time series (from left to right) on an existing building in Osaka, Japan. It can be observed that plastic torsional deformations are accumulated over time. It is worth noting that the plan of the building is symmetrical and concentric and only horizontal translational ground motion is applied in the direction diagonal to the principal axis.

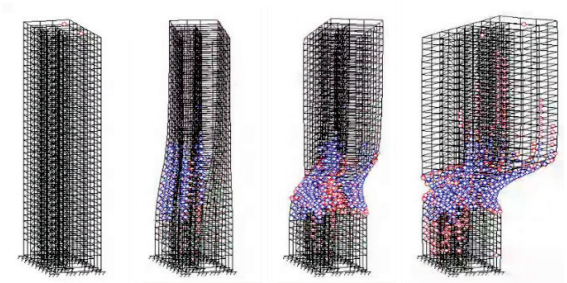

Fig.1 Snapshots of time history response analysis
(Courtesy of Professor Yoshikazu Araki of Nagoya University)

No special consideration of the torsional vibration of the structure was required in the structural design because the plan of the building is symmetrical and concentric.

The building was built in the early 1990s. Before the 1995 Kobe Earthquake, the minimum requirement for the PGV of the design ground motion at the building site was 80% of the current requirement and a PGV of 0.4 m/s was used for the maximum considerable input level, which is not considered enough after experiencing the Kobe and Tohoku Earthquakes. The input ground motion employed in the combined non-linear analysis is a scenario-based synthetic ground motion of the hypothetical Nankai Mega-thrust Earthquake. The torsional collapse behavior is observed when the amplitude of the ground motion is scaled by 105% and applied in the direction of 45 degrees from the principal axis of the building.

In Fig.1, we can observe that all the beam ends of both the longitudinal and transverse frames in the lower stories yield, creating unstable status, and thus resulting in accumulated torsional deformation. Uemura and Uetani [8] pointed out that this phenomenon has similarity with DCILS and elucidated that it was bifurcation type inelastic buckling. Indeed, the torsional buckling mechanism is found to have similarity with Shanley's inelastic column theory [9]. They investigate a one-story symmetric and concentric cubic frame model in which only the torsional stiffness remains even after all the beam ends yield. They also derived equilibrium equations and performed load-control analysis with a horizontal load at the rooftop in a direction diagonal to the principal axis. The deformation orthogonal to the loading direction is fixed for simplicity. They find that bifurcation to the torsional direction can occur in a symmetric and concentric frame if the torsional stiffness is smaller than a specific value.

In a previous research [10], we conducted a load-controlled analysis on the present model, in which orthogonal deformation remained free, and horizontal post-yielding stiffness remained positive unlike the study conducted by Uemura and Uetani. This study further aims to reveal the occurrence conditions of inelastic torsional buckling in a high-rise steel moment resisting frame (SMRF) considering non-zero post-yielding stiffness, and investigates the special case where the horizontal and torsional post-yielding stiffness remains positive while the torsional and horizontal stiffness become zero at the singular point. The uniqueness of a rate

solution is examined using the concept of the comparison solid proposed by Hill [11-15]. Moreover, we investigate the consistency of the stiffness in some critical cases regarding the post-bifurcation behavior.

2. Analytical Model and Method

2.1 Analytical Model

Fig.2 depicts the one-story simple symmetric and concentric cube frame model subjected to horizontal force at the center of gravity on the roof, which is the same as the model in previous research [10]. It has two couples of horizontal elastic springs in the X and Y directions. The stiffness of each spring is $K/2$, and each is located at a distance e from the center of gravity. Each column is pin supported. The span is a in each direction, and the story height is h. The flexibility of the frame is represented by rotational springs at the beam ends. Thus, the elements between the ends of the beams and columns are modeled as rigid bodies. The rotational springs at the beam ends have perfect elastic-plastic restoring-force characteristics with an elastic stiffness of k. The roof serves as a rigid diaphragm. The frames of the model are numbered from (1) to (4), as shown in Fig.2. The vertical load W, acts on the top of each column, and a horizontal load H, is applied at the center of the roof in the direction 45° from the X-axis. The horizontal displacements in the directions parallel and orthogonal to the loading direction are u and v, respectively. The rotational displacement angle of the roof is θ.

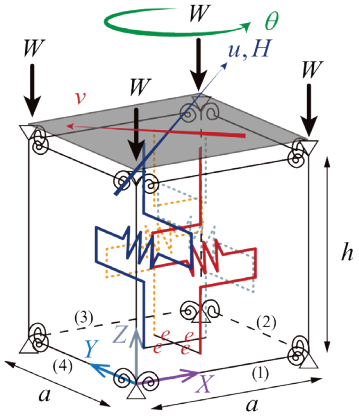

Fig.2 One-story simple symmetric cube frame model

In this model, post-yielding horizontal stiffness K_{Gh} and torsional stiffness K_{Gr} are expressed in Eq. (1)

$$K_{Gh} = K - \frac{4W}{h},\quad K_{Gr} = 2Ke^2 - \frac{2a^2W}{h} \tag{1}$$

The second terms represent the P-Delta effect.

2.2 Method

This is a simple model of a high-rise building whose beam ends in lower stories yield as depicted in Fig. 3, where h represents the height of the inelastic region.

In the previous research, post-yield stiffness K_{Gh} and K_{Gr} are the critical factors of the occurrence of this phenomenon. Typically, it is expected for the stiffness K and vertical load W to decrease if the plastic region expands upwards; therefore, h can be considered as a path parameter of bifurcation analysis. In this study, we set h as the path parameter and assume that K_{Gh} and K_{Gr} monotonically decrease as h increases.

Whereas we conducted a load-control analysis for the case of $K_{Gh} > 0$ in the former report, we conduct displacement-control analysis with the control parameter $\dot{u}$ to avoid instability at the singular point.

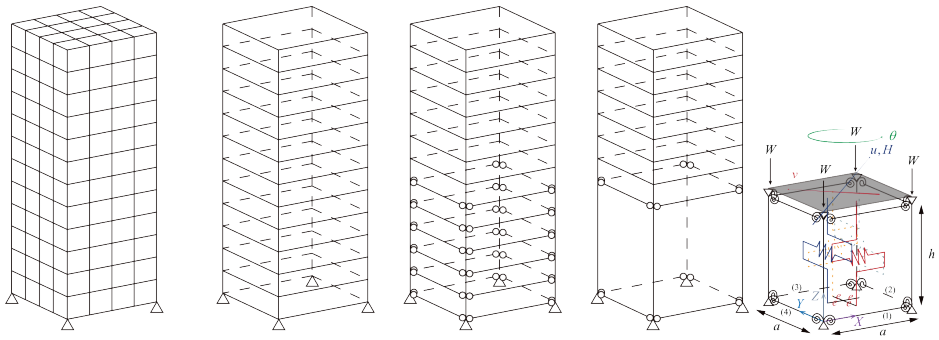

(a) (b) (c) (d) (e)

Fig. 3 Detail of the modeling

3. Fundamental Equations

3.1 Compatibility condition equations

Let i be the number of the frame, and the angle of the beam-end rotation of the frame i be defined as φ_i . The deformations u, v, θ, φ_i are assumed to be infinitesimal, and therefore, approximations, $\sin\theta(\varphi_i) \approx \theta(\varphi_i)$, $\cos\theta(\varphi_i) \approx 1$, hold.

φ_i is expressed as follows, Eq.(2).

$$\begin{cases} \varphi_1 = \dfrac{1}{h}\left(\dfrac{1}{\sqrt{2}}u - \dfrac{1}{\sqrt{2}}v + \dfrac{a}{2}\theta\right) \\ \varphi_2 = \dfrac{1}{h}\left(\dfrac{1}{\sqrt{2}}u + \dfrac{1}{\sqrt{2}}v + \dfrac{a}{2}\theta\right) \\ \varphi_3 = \dfrac{1}{h}\left(\dfrac{1}{\sqrt{2}}u - \dfrac{1}{\sqrt{2}}v - \dfrac{a}{2}\theta\right) \\ \varphi_4 = \dfrac{1}{h}\left(\dfrac{1}{\sqrt{2}}u + \dfrac{1}{\sqrt{2}}v - \dfrac{a}{2}\theta\right) \end{cases} \tag{2}$$

3.2 Equilibrium equations

Let Q_i be the shear force of the i^{th} frame, and M_i be its beam-end bending moment.

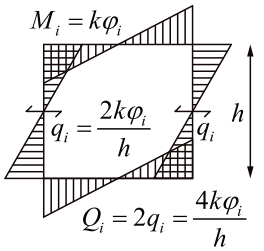

Fig.4 Moment diagram of the frames

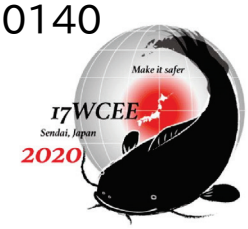

Fig.4 shows the moment diagram of the frame i, and thus Q_i and M_i satisfy the following relations. The equilibrium equations at the roof level can then be expressed as follows;

$$\begin{cases} Q_i = \dfrac{4M_i}{h} \\ \text{u-axis}: \quad \dfrac{1}{\sqrt{2}}\left(Q_1+Q_2+Q_3+Q_4\right)+K_{Gh}\cdot u = H \\ \text{v-axis}: \quad \dfrac{1}{\sqrt{2}}\left(-Q_1+Q_2-Q_3+Q_4\right)+K_{Gh}\cdot v = 0 \\ \theta\text{-axis}: \quad \dfrac{a}{2}\left(Q_1+Q_2-Q_3-Q_4\right)+K_{Gr}\cdot \theta = 0 \end{cases} \tag{3}$$

4. Rate Solutions

4.1 Fundamental Path

The rate solutions of the fundamental path, which is represented by the superscript $(\ )^f$, are given below.

$$\dot{u}^f = {}^{\forall}\dot{u}\left(\text{controlled parameter}\right),\ \dot{v}^f = 0,\ \dot{\theta}^f = 0 \tag{4}$$

$$\begin{cases} \text{u-axis}: \quad \dfrac{1}{\sqrt{2}}\left(\dot{Q}_1^f+\dot{Q}_2^f+\dot{Q}_3^f+\dot{Q}_4^f\right)+K_{Gh}\cdot\dot{u}^f = \dot{H} \\ \text{v-axis}: \quad \dfrac{1}{\sqrt{2}}\left(-\dot{Q}_1^f+\dot{Q}_2^f-\dot{Q}_3^f+\dot{Q}_4^f\right)+K_{Gh}\cdot\dot{v}^f = 0 \\ \theta\text{-axis}: \quad \dfrac{a}{2}\left(\dot{Q}_1^f+\dot{Q}_2^f-\dot{Q}_3^f-\dot{Q}_4^f\right)+K_{Gr}\cdot\dot{\theta}^f = 0 \end{cases} \tag{5}$$

$$\dot{\varphi}_i^f = \frac{\dot{u}^f}{\sqrt{2}h}\quad (i=1,2,3,4),\ \dot{Q}_i^f = \begin{cases} \dfrac{4k\dot{\varphi}_i^f}{h} = \dfrac{2\sqrt{2}}{h^2}\dot{u}^f & \left(\text{for elastic or unloading}\right) \\ 0 & \left(\text{for loading}\right) \end{cases} \tag{6}$$

4.2 Bifurcation Path

The rate solutions of the bifurcation path, which is represented by the superscript $(\ )^b$, are given below.

$$\begin{cases} \dot{\varphi}_1^b = \dfrac{1}{h}\left(\dfrac{1}{\sqrt{2}}\dot{u}^b-\dfrac{1}{\sqrt{2}}\dot{v}^b+\dfrac{a}{2}\dot{\theta}^b\right) \\ \dot{\varphi}_2^b = \dfrac{1}{h}\left(\dfrac{1}{\sqrt{2}}\dot{u}^b+\dfrac{1}{\sqrt{2}}\dot{v}^b+\dfrac{a}{2}\dot{\theta}^b\right) \\ \dot{\varphi}_3^b = \dfrac{1}{h}\left(\dfrac{1}{\sqrt{2}}\dot{u}^b-\dfrac{1}{\sqrt{2}}\dot{v}^b-\dfrac{a}{2}\dot{\theta}^b\right) \\ \dot{\varphi}_4^b = \dfrac{1}{h}\left(\dfrac{1}{\sqrt{2}}\dot{u}^b+\dfrac{1}{\sqrt{2}}\dot{v}^b-\dfrac{a}{2}\dot{\theta}^b\right) \end{cases} \quad \begin{cases} \text{u-axis}: \quad \dfrac{1}{\sqrt{2}}\left(\dot{Q}_1^b+\dot{Q}_2^b+\dot{Q}_3^b+\dot{Q}_4^b\right)+K_{Gh}\cdot\dot{u}^b = \dot{H} \\ \text{v-axis}: \quad \dfrac{1}{\sqrt{2}}\left(-\dot{Q}_1^b+\dot{Q}_2^b-\dot{Q}_3^b+\dot{Q}_4^b\right)+K_{Gh}\cdot\dot{v}^b = 0 \\ \theta\text{-axis}: \quad \dfrac{a}{2}\left(\dot{Q}_1^b+\dot{Q}_2^b-\dot{Q}_3^b-\dot{Q}_4^b\right)+K_{Gr}\cdot\dot{\theta}^b = 0 \end{cases} \tag{7}$$

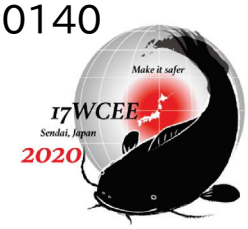

5 Uniqueness of Rate Solution

5.1 Sufficient Condition

The concept of Hill's comparison solid [11-15] is applied to examine the uniqueness of the rate solutions. Following the same procedure performed in the previous study [10] obtains;

$$\Omega\left(\dot{\mathbf{u}}^{b},\dot{\mathbf{u}}^{f}\right)=0 \tag{8}$$

where

$$\dot{\mathbf{u}}^{*}\equiv\left(\dot{u}^{*},\dot{v}^{*},\dot{\theta}^{*}\right)$$

$$\dot{\mathbf{u}}^{*}\equiv\left(\dot{u}^{*},\dot{v}^{*},\dot{\theta}^{*}\right),\ \Omega\left(\dot{\mathbf{u}},\dot{\mathbf{u}}^{*}\right)\equiv\sum_{i=1}^{4}\left(\dot{Q}_{i}-\dot{Q}_{i}^{*}\right)h\left(\dot{\varphi}_{i}-\dot{\varphi}_{i}^{*}\right)+K_{Gh}\left\{\left(\dot{u}-\dot{u}^{*}\right)^{2}+\left(\dot{v}-\dot{v}^{*}\right)^{2}\right\}+K_{Gr}\left(\dot{\theta}-\dot{\theta}^{*}\right)^{2} \tag{9}$$

The function $\Omega\left(\dot{\mathbf{u}},\dot{\mathbf{u}}^{*}\right)$ corresponds to the functional $\Sigma\left(\dot{\mathbf{u}},\dot{\mathbf{u}}^{*}\right)$ defined by Hill [11-15].

If a bifurcation occurs from a particular equilibrium state on the fundamental path, there exists a rate solution on the bifurcation path that satisfies Eq.(8). The contraposition demands that bifurcations never occur from the equilibrium state of interest if any rate solution $\dot{\mathbf{u}}$ other than $\dot{\mathbf{u}}^{f}$ violates the condition of Eq.(8). Therefore, the sufficient condition for the uniqueness of the rate solution is expressed as follows:

$$^{\forall}\dot{\mathbf{u}}\neq\dot{\mathbf{u}}^{f},\ \Omega\left(\dot{\mathbf{u}},\dot{\mathbf{u}}^{f}\right)\neq 0\Rightarrow\dot{\mathbf{u}}^{f}\ \text{is unique.} \tag{10}$$

As mentioned in Section 2.2, usually, it is expected for the stiffness K to decrease if the plastic region h expands upwards. We assume that the same thing applies to K_{Gh} and K_{Gr}, *i.e.*, they monotonically decrease as h increases. Additionally, the vertical load which influences the P-Delta effect is the largest at first. For simplicity, let us confine ourselves to the case in which post-yielding stiffness remains positive in the region around the bifurcation point.

$$K_{Gh}>0,K_{Gr}>0 \tag{11}$$

Under this assumption, consequently, $\Omega\left(\dot{\mathbf{u}},\dot{\mathbf{u}}^{f}\right)$ is non-negative. The sufficient condition for the uniqueness is relaxed to the following:

$$^{\forall}\dot{\mathbf{u}}\neq\dot{\mathbf{u}}^{f},\ \Omega\left(\dot{\mathbf{u}},\dot{\mathbf{u}}^{f}\right)>0\Rightarrow\dot{\mathbf{u}}^{f}\ \text{is unique.} \tag{12}$$

Furthermore, by replacing $\dot{\mathbf{u}}^{f}$ with any rate vector $\dot{\mathbf{u}}^{*}$ including $\dot{\mathbf{u}}^{f}$, we obtain a further relaxed sufficient condition as follows:

$$^{\forall}\dot{\mathbf{u}}\neq\dot{\mathbf{u}}^{*},\ \Omega\left(\dot{\mathbf{u}},\dot{\mathbf{u}}^{*}\right)>0\Rightarrow\dot{\mathbf{u}}^{*}\ \text{is unique.} \tag{13}$$

Here, we assume that all the beam-end springs are in the loading state and thus $\dot{M}_{i}=\dot{Q}_{i}=0\ \left(i=1,2,3,4\right)$, following the concept of Hill's comparison solid [11-15]. The modified function of Eq.(9), can be defined as follows:

$$\Omega^{he}\left(\dot{\mathbf{u}},\dot{\mathbf{u}}^{*}\right)\equiv K_{Gh}\left\{\left(\dot{u}-\dot{u}^{*}\right)^{2}+\left(\dot{v}-\dot{v}^{*}\right)^{2}\right\}+K_{Gr}\left(\dot{\theta}-\dot{\theta}^{*}\right)^{2} \tag{14}$$

Obviously,

$$\Omega\left(\dot{\mathbf{u}},\dot{\mathbf{u}}^{*}\right)>\Omega^{he}\left(\dot{\mathbf{u}},\dot{\mathbf{u}}^{*}\right) \tag{15}$$

Hence, the sufficient condition for the uniqueness of the rate solution, Eq.(12), is further relaxed.

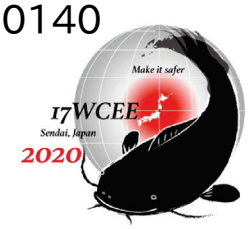

$$^{\forall}\dot{\mathbf{u}} \neq \dot{\mathbf{u}}^{*},\ \Omega^{he}\left(\dot{\mathbf{u}},\dot{\mathbf{u}}^{*}\right) > 0 \Rightarrow \dot{\mathbf{u}}^{*} \text{ is unique.} \tag{16}$$

Substituting $\dot{\mathbf{u}}^{f}$ for $\dot{\mathbf{u}}^{*}$ into Eq.(16) yields the following, conclusively:

$$^{\forall}\dot{\mathbf{u}} \neq \dot{\mathbf{u}}^{f},\ \Omega^{he}\left(\dot{\mathbf{u}},\dot{\mathbf{u}}^{f}\right) = K_{Gh}\left\{\left(\dot{u}-\dot{u}^{f}\right)^{2}+\left(\dot{v}-\dot{v}^{f}\right)^{2}\right\}+K_{Gr}\left(\dot{\theta}-\dot{\theta}^{f}\right)^{2} > 0 \Rightarrow \dot{\mathbf{u}}^{f} \text{ is unique.} \tag{17}$$

5.2 Bifurcation

Violation of the sufficient condition for the uniqueness of the rate solution means that bifurcation can occur. As h increases, bifurcation can occur in the following three cases: (1) K_{Gh} remains positive, but K_{Gr} reaches zero. (2) K_{Gr} remains positive, but K_{Gh} reaches zero (3) K_{Gh} and K_{Gr} reach zero at the same time. In the following sub-sections, each case is examined in detail.

5.2.1 $K_{Gh} > 0,\ K_{Gr} = 0$

Sufficient condition, Eq.(17), is as follows:

$$^{\forall}\dot{\mathbf{u}} \neq \dot{\mathbf{u}}^{f},\ \Omega^{he}\left(\dot{\mathbf{u}},\dot{\mathbf{u}}^{f}\right) = K_{Gh}\left\{\left(\dot{u}-\dot{u}^{f}\right)^{2}+\left(\dot{v}-\dot{v}^{f}\right)^{2}\right\} > 0 \Rightarrow \dot{\mathbf{u}}^{f} \text{ is unique.} \tag{18}$$

From the assumption of $K_{Gh} > 0$, the violation of the sufficient condition demands the following:

$$\dot{\mathbf{u}} = \left(\dot{u}^{f},\ \dot{v}^{f},\ ^{\forall}\dot{\theta}\right) = \left(^{\forall}\dot{u},\ 0,\ ^{\forall}\dot{\theta}\right) \neq \dot{\mathbf{u}}^{f} \tag{19}$$

5.2.2 $K_{Gh} = 0,\ K_{Gr} > 0$

Sufficient condition, Eq.(17), is as follows:

$$^{\forall}\dot{\mathbf{u}} \neq \dot{\mathbf{u}}^{f},\ \Omega^{he}\left(\dot{\mathbf{u}},\dot{\mathbf{u}}^{f}\right) = K_{Gr}\left(\dot{\theta}-\dot{\theta}^{f}\right)^{2} > 0 \Rightarrow \dot{\mathbf{u}}^{f} \text{ is unique.} \tag{20}$$

From the assumption of $K_{Gr} > 0$, the violation of the sufficient condition demands the following:

$$\dot{\mathbf{u}} = \left(^{\forall}\dot{u},\ ^{\forall}\dot{v},\ \dot{\theta}^{f}\right) = \left(^{\forall}\dot{u},\ ^{\forall}\dot{v},\ 0\right) \neq \dot{\mathbf{u}}^{f} \tag{21}$$

5.2.2 $K_{Gh} = 0,\ K_{Gr} = 0$

In this case, $\Omega^{he}\left(\dot{\mathbf{u}},\dot{\mathbf{u}}^{*}\right) = 0$ always, and thus the violation of the sufficient condition demands the following:

$$^{\forall}\dot{\mathbf{u}} \neq \dot{\mathbf{u}}^{f} \tag{22}$$

Table 1 summarizes the results above.

Table 1 – Solutions that break the sufficient condition of the uniqueness.

		K_{Gr}	
		>0	=0
K_{Gh}	>0	None.	$\dot{\mathbf{u}} = \left(\dot{u}^{f},\ \dot{v}^{f},\ ^{\forall}\dot{\theta}\right) = \left(^{\forall}\dot{u},\ 0,\ ^{\forall}\dot{\theta}\right) \neq \dot{\mathbf{u}}^{f}$
	=0	$\dot{\mathbf{u}} = \left(^{\forall}\dot{u},\ ^{\forall}\dot{v},\ \dot{\theta}^{f}\right) = \left(^{\forall}\dot{u},\ ^{\forall}\dot{v},\ 0\right) \neq \dot{\mathbf{u}}^{f}$	$^{\forall}\dot{\mathbf{u}} \neq \dot{\mathbf{u}}^{f}$

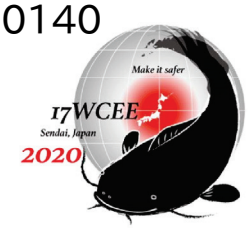

6. Consistency of Post-Bifurcation Behavior

16 combinations exist depending on whether each $\dot{\varphi}_i$ is in the elastic/unloading [E] or loading [P] states. Each combination is represented by [E/P, E/P, E/P, E/P], wherein each component corresponds to the state of $\dot{\varphi}_1$, $\dot{\varphi}_2$, $\dot{\varphi}_3$, $\dot{\varphi}_4$, respectively.

Previous research [10] proved that the [P, P, P, P] and [P, P, E, E] states as well as [E, E, P, P] state that are symmetric to the [P, P, E, E] state satisfied the consistency of the loading states when the horizontal post-yield stiffness K_{Gh} remained positive. In this study, we discuss the case of [P, P, P, P], [P, P, E, E], and [P, E, P, E] states, in the limited cases where K_{Gh} or K_{Gr} remain positive, and K_{Gh} and K_{Gr} are zero at the same time, as shown in Table 2. The other cases, *e.g.*, [E, P, P, P] state, where K_{Gh} and K_{Gr} are negative at the same time, and so on, are saved for future work.

Table 2 – Cases discussed in this paper, i–v)

		K_{Gr}		
		>0	=0	<0
K_{Gh}	>0	None.	i)	ii)
	=0	iii)	iv)	
	<0	v)		

6.1 [P, P, P, P] state

The equilibrium equations are expressed as follows;

$$\text{u-axis}: K_{Gh}\cdot\dot{u}=\dot{H},\ \text{v-axis}: K_{Gh}\cdot\dot{v}=0,\ \theta\text{-axis}: K_{Gr}\cdot\dot{\theta}=0 \tag{23}$$

Indeterminate consistent solutions exist in cases i), iii) and iv).

6.1.1 $K_{Gh}>0,\ K_{Gr}=0$

Eq.(23) can be solved as follows:

$$\dot{\mathbf{u}}=\left({}^{\forall}\dot{u},\ 0,\ {}^{\forall}\dot{\theta}\right)\neq\dot{\mathbf{u}}^{f}\cap\dot{H}=K_{Gh}\cdot{}^{\forall}\dot{u} \tag{24}$$

Then, we have Eq.(25) that satisfies the consistency

$$\dot{\varphi}_1=\dot{\varphi}_2=\frac{1}{h}\left(\frac{1}{\sqrt{2}}\dot{u}+\frac{a}{2}\dot{\theta}\right)\geq 0\cap\dot{\varphi}_3=\dot{\varphi}_4=\frac{1}{h}\left(\frac{1}{\sqrt{2}}\dot{u}-\frac{a}{2}\dot{\theta}\right)\geq 0\,. \tag{25}$$

It follows that,

$$-\sqrt{2}\dot{u}/a\leq\dot{\theta}\leq\sqrt{2}\dot{u}/a\,. \tag{26}$$

To avoid Eq.(26) becoming an empty set, we have $\dot{u}>0$, and thus we obtain the following indeterminate solution.

$$-\sqrt{2}\dot{u}/a\leq\dot{\theta}\leq\sqrt{2}\dot{u}/a,\ \dot{u}>0\,. \tag{27}$$

6.1.2 $K_{Gh}=0,\ K_{Gr}>0$

Eq.(23) can be solved as follows.

$$\dot{\mathbf{u}} = \left({}^{\forall}\dot{u},\ {}^{\forall}\dot{v},\ 0 \right) \neq \dot{\mathbf{u}}^{f} \cap \dot{H} = 0 \tag{28}$$

It follows that,

$$\dot{\varphi}_1 = \dot{\varphi}_3 = \frac{1}{h}\left(\frac{1}{\sqrt{2}}\dot{u} - \frac{1}{\sqrt{2}}\dot{v} \right) \geq 0 \cap \dot{\varphi}_2 = \dot{\varphi}_4 = \frac{1}{h}\left(\frac{1}{\sqrt{2}}\dot{u} + \frac{1}{\sqrt{2}}\dot{v} \right) \geq 0 . \tag{29}$$

By following the same procedure described in 6.1.1 and from Eq.(29), we obtain the following indeterminate solution,

$$-\dot{u} \leq \dot{v} \leq \dot{u},\ \ \dot{u} > 0 . \tag{30}$$

6.1.3 $K_{Gh} = 0,\ K_{Gr} = 0$

Solutions of Eq.(23) are as follows;

$${}^{\forall}\dot{\mathbf{u}} \neq \dot{\mathbf{u}}^{f} \cap \dot{H} = 0 \tag{31}$$

We then have indeterminate solutions of Eq.(32) that satisfy the consistency

$$\begin{cases} \dot{\varphi}_1 = \dfrac{1}{h}\left(\dfrac{1}{\sqrt{2}}\dot{u} - \dfrac{1}{\sqrt{2}}\dot{v} + \dfrac{a}{2}\dot{\theta} \right) \geq 0 \\ \dot{\varphi}_2 = \dfrac{1}{h}\left(\dfrac{1}{\sqrt{2}}\dot{u} + \dfrac{1}{\sqrt{2}}\dot{v} + \dfrac{a}{2}\dot{\theta} \right) \geq 0 \\ \dot{\varphi}_3 = \dfrac{1}{h}\left(\dfrac{1}{\sqrt{2}}\dot{u} - \dfrac{1}{\sqrt{2}}\dot{v} - \dfrac{a}{2}\dot{\theta} \right) \geq 0 \\ \dot{\varphi}_4 = \dfrac{1}{h}\left(\dfrac{1}{\sqrt{2}}\dot{u} + \dfrac{1}{\sqrt{2}}\dot{v} - \dfrac{a}{2}\dot{\theta} \right) \geq 0 \end{cases} \Leftrightarrow \begin{cases} \dot{v} \leq \dfrac{a}{\sqrt{2}}\dot{\theta} + \dot{u} \\ \dot{v} \geq -\dfrac{a}{\sqrt{2}}\dot{\theta} - \dot{u} \\ \dot{v} \leq -\dfrac{a}{\sqrt{2}}\dot{\theta} + \dot{u} \\ \dot{v} \geq \dfrac{a}{\sqrt{2}}\dot{\theta} - \dot{u} \end{cases} \tag{32}$$

To avoid Eq.(32) becoming an empty set, we have $\dot{u} > 0$.

6.2 [P, P, E, E] (neutral loading) state

The equilibrium equations are as follows;

$$\text{u-axis}:\left(K_{Gh} + \frac{4k}{h^2} \right)\dot{u} - \frac{2\sqrt{2}ak}{h^2} = \dot{H},\ \ \text{v-axis}:\left(K_{Gh} + \frac{4k}{h^2} \right)\dot{v} = 0,\ \ \theta\text{-axis}:-\frac{2\sqrt{2}ak}{h^2}\dot{u} + \left(K_{Gr} + \frac{2a^2k}{h^2} \right)\dot{\theta} = 0 \tag{33}$$

The indeterminate solution exists in case ii), and unique solutions exist in cases ii), iv), and v).

6.2.1 $K_{Gh} > 0,\ K_{Gr} < 0$ (and $K_{Gh} < 0, K_{Gr} > 0$)

Except for the singular point of $d_{PPEE} = 0$, Eq.(33) obtains unique solutions as follows;

$$\dot{u} = \frac{\left(2a^2k + h^2K_{Gr} \right)\dot{H}}{d_{PPEE}} \cap \dot{v} = 0 \cap \dot{\theta} = \frac{2\sqrt{2}ak\dot{H}}{d_{PPEE}} = \frac{2a^2k}{2a^2k + h^2K_{Gr}} \cdot \frac{\sqrt{2}}{a}\dot{u} , \tag{34}$$

where, $d_{PPEE} = 2a^2kK_{Gh} + h^2K_{Gh}K_{Gh} + 4kK_{Gr}K$, and provided that $d_{PPEE} \neq 0$, we have,

$$\dot{\varphi}_1 = \dot{\varphi}_2 = \frac{\left(4a^2k + h^2K_{Gr} \right)\dot{H}}{\sqrt{2}hd_{PPEE}} \geq 0 \cap \dot{\varphi}_3 = \dot{\varphi}_4 = \frac{hK_{Gr}\dot{H}}{\sqrt{2}d_{PPEE}} < 0 . \tag{35}$$

From the condition $K_{Gr} < 0$, we obtain the following;

$$\dot{u}>0,\ -2a^2k/h^2<K_{Gr}<0\cup\dot{u}<0,\ -4a^2k/h^2\le K_{Gr}<-2a^2k/h^2 \tag{36}$$

If the condition represented in Eq.(36) is satisfied, there exists the unique solution, Eq.(34), and

$$\dot{\theta}=2a^2k/\left(2a^2k+h^2K_{Gr}\right)\cdot\sqrt{2}\dot{u}/a>\sqrt{2}\dot{u}/a\ \ (\text{for }\dot{u}>0)\ \text{ or }\ -\sqrt{2}\dot{u}/a\ \ (\text{for }\dot{u}<0). \tag{37}$$

One singular solution is an exception of Eq.(36), *i.e.* $K_{Gr}=-2a^2k/h^2\cap\dot{u}=0$. In this case, we obtain indeterminate solution as follows;

$$^{\forall}\dot{H}<0\cap\dot{\theta}=-h^2\dot{H}/2\sqrt{2}ak>0 \tag{38}$$

Another singular solution is in the case where $d_{PPEE}=0$ and this case gives the following;

$$d_{PPEE}=0\Leftrightarrow K_{Gh}=-\frac{4kK_{Gr}}{2a^2k+h^2K_{Gr}}\cap-\frac{2a^2k}{h^2}<K_{Gr}<0\cap\left(\dot{u}>0,\ \dot{\theta}>\frac{\sqrt{2}}{a}\dot{u}\cup\dot{u}<0,\ \dot{\theta}\ge-\frac{\sqrt{2}}{a}\dot{u}\right) \tag{39}$$

The last condition include the singular solution of case v), $K_{Gh}<0,K_{Gr}>0$, but the region of K_{Gh} differs; practically, we obtain the following in case v);

$$d_{PPEE}=0\Leftrightarrow K_{Gr}=-\frac{2a^2kK_{Gh}}{h^2K_{Gh}+4k}\cap-\frac{4k}{h^2}<K_{Gh}<0\cap\left(\dot{u}>0,\ \dot{\theta}>\frac{\sqrt{2}}{a}\dot{u}\cup\dot{u}<0,\ \dot{\theta}\ge-\frac{\sqrt{2}}{a}\dot{u}\right) \tag{40}$$

6.2.2 $K_{Gh}=0,\ K_{Gr}=0$

$\dot{H}=0\cap\dot{\mathbf{u}}=\left(^{\forall}\dot{u},\ 0,\ ^{\forall}\dot{\theta}\right)$ is the indeterminate solution of Eq.(33), and it gives the following condition;

$$\dot{u}>0,\ \dot{\theta}>\sqrt{2}\dot{u}/a\cup\dot{u}<0,\ \dot{\theta}\ge-\sqrt{2}\dot{u}/a \tag{41}$$

6.3 [P, E, P, E] (neutral loading) state

The equilibrium equations are as follows.

$$\text{u-axis}:\left(K_{Gh}+\frac{4k}{h^2}\right)\dot{u}+\frac{4k}{h^2}\dot{v}=\dot{H},\ \ \text{v-axis}:\frac{4k}{h^2}\dot{u}+\left(K_{Gh}+\frac{4k}{h^2}\right)\dot{v}=0,\ \ \theta\text{-axis}:\left(K_{Gr}+\frac{2a^2k}{h^2}\right)\dot{\theta}=0 \tag{42}$$

There exist consistent solutions only in case v), $K_{Gh}<0,\ K_{Gr}>0$.

6.3.1 $K_{Gh}<0,\ K_{Gr}>0$

The case has two solutions, one is the general unique solution, and the other is the singular solution. First, we look at the general solutions. Provided that $K_{Gh}\neq-8k/h^2$, Eq.(42) can be solved as follows;

$$\dot{u}=\frac{\left(h^2K_{Gh}+4k\right)\dot{H}}{K_{Gh}\left(h^2K_{Gh}+8k\right)}\cap\dot{v}=-\frac{4k\dot{H}}{K_{Gh}\left(h^2K_{Gh}+8k\right)}\cap\dot{\theta}=0 \tag{43}$$

It follows that,

$$\dot{\varphi}_1=\dot{\varphi}_3=\frac{\dot{H}}{\sqrt{2}hK_{Gh}}\ge0\cap\dot{\varphi}_2=\dot{\varphi}_4=\frac{h\dot{H}}{\sqrt{2}\left(h^2K_{Gh}+8k\right)}<0. \tag{44}$$

From the condition $K_{Gh}<0$, we obtain the following;

$$\dot{H}<0\cap\left(-\frac{4k}{h^2}<K_{Gh}<0,\ \dot{u}>0\cup-\frac{8k}{h^2}<K_{Gh}<-\frac{4k}{h^2},\ \dot{u}<0\right) \tag{45}$$

If the condition represented in Eq.(45), was satisfied, there exists the unique solution Eq.(43), and

$$\dot{v} = -\frac{4k}{h^2 K_{Gh} + 4k}\dot{u} < -\dot{u} \quad (\text{for } \dot{u} > 0) \text{ or } \dot{u} \quad (\text{for } \dot{u} < 0). \tag{46}$$

If $\dot{H} = 0$, the case $K_{Gh} = -4k/h^2 \cap \dot{u} = 0$ has a solution, but it is the same as $\dot{\mathbf{u}}^f$; thus, we can exclude it.

Another singular solution is obtained in the case where $K_{Gh} = -8k/h^2$. Eq.(42) can be solved as follows;

$$\dot{H} = 0, \ \dot{v} = \dot{u}, \ \dot{\theta} = 0 \tag{47}$$

It follows that,

$$\dot{\varphi}_1 = \dot{\varphi}_3 = 0 \geq 0 \cap \dot{\varphi}_2 = \dot{\varphi}_4 = \sqrt{2}\dot{v} < 0. \tag{48}$$

From Eq.(48), we obtain $\dot{u} < 0$, and if this condition is satisfied, Eq.(47) is confirmed to be a consistent solution.

6.4 Discussion

Summarizing Eqs.(27),(30),(32),(37),(38),(39),(40),(41),(46) and (47) gives Fig.5.

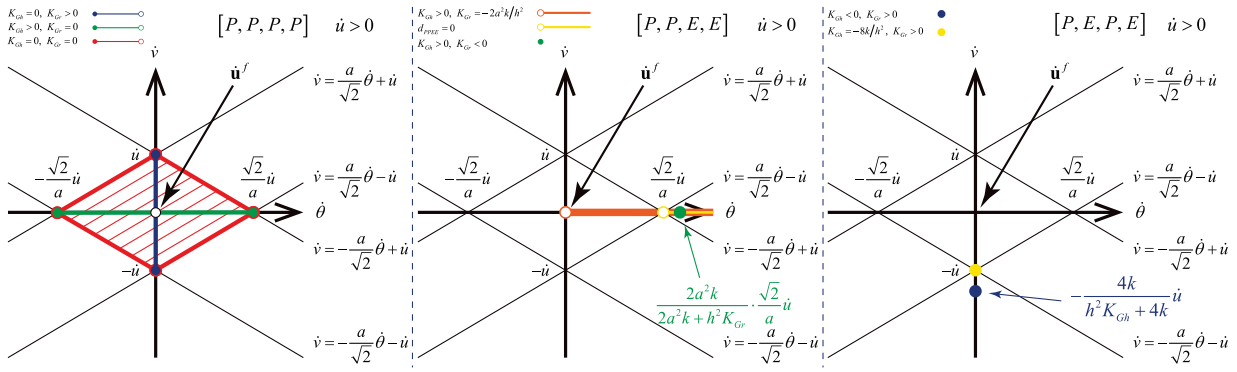

(a) [P,P,P,P] (b) [P,P,E,E] (neutral loading) (c) [P,E,P,E] (neutral loading)

Fig. 5 Behavior in each state.

As a typical behavior, let us assume the case where $\dot{u}$ is a positive constant, as the path parameter h increases, K_{Gr} decreases. When K_{Gr} reaches 0, the uniqueness of the rate solution is violated and bifurcation occurs (indicated by green-line in Fig.5(a)). When K_{Gr} decreases further to a negative value, the frame gets in the neutral loading state [P, P, E, E] and $\dot{\theta}$ has a unique solution (indicated by green filled circle in Fig.5(b)) in accordance with the value of K_{Gr}. Although further thorough investigation is needed, it is worth noting that the transition from the [P, P, P, P] state where $K_{Gh} > 0, \ K_{Gr} = 0$ to the [P, P, E, E] state where $K_{Gh} > 0, \ K_{Gr} < 0$ is continuous at $\dot{\mathbf{u}} = \left(\dot{u}, 0, a\dot{u}/\sqrt{2}\right)$.

6. Conclusion

To reveal the occurrence conditions of inelastic torsional buckling in a high-rise steel moment resisting frame considering non-negative post-yielding stiffness, we employed a simple cubic frame model, conducted deformation-control analysis, discussed the uniqueness of the rate solution using the concept of the comparison solid proposed by Hill, and investigated the consistency of post-bifurcation behavior. It was elucidated that a perfectly symmetric and concentric frame subjected to only horizontal translational loading can bifurcate to exhibit torsional deformation explaining the accumulation of torsional deformation observed in the time history analysis of an existing concentric high-rise building subjected to horizontal ground motion.

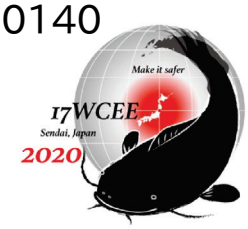

Acknowledgments

The authors are grateful to Emeritus Professor Koji Uetani of Kyoto University for his valuable suggestions in preparing this paper. The snapshots of the seismic response deformations of the high-rise building are provided courtesy of Professor Yoshikazu Araki of Nagoya University, which is highly appreciated.

References

[1] Tsurugi M, Zhao B, Petukhin A, Kagawa T (2005): Strong Ground Motion Prediction in Osaka Prefecture during the Nankai and Tonankai Earthquake. *Journal of Structural Engineering A,* **51A** (501–512.

[2] Kashima T, Koyama S, Okawa I (2012): Strong Motion Records in Buildings from the 2011 off the Pacific coast of Tohoku Earthquake. *BRI Research Data 135*, Building Research Institute Incorporated Administrative Agency (BRI), Japan.

[3] Atwater BF, Nelson AR, Clague JJ, Carver GA, Yamaguchi DK, Bobrowsky PT, Bourgeois J, Darienzo ME, Grant WC, Hemphill-Haley E, Kelsey HM, Jacoby GC, Nishenko SP, Palmer SP, Peterson CD, Reinhart MA (1995): Summary of Coastal Geologic Evidence for past Great Earthquakes at the Cascadia Subduction Zone. *Earthquake Spectra,* **11**(1), 1–18.

[4] Goldfinger C, Nelson CH, Morey AE, Johnson JE, Patton JR, Karabanov EB, Gutierrez-Pastor J, Eriksson AT, Gracia E, Dunhill G, Enkin RJ, Dallimore A, Vallier T (2012): Turbidite event history—Methods and Implications for Holocene Paleoseismicity of the Cascadia Subduction Zone. *Professional Paper 1661F*, Reston, VA, USA.

[5] Petersen MD, Cramer CH, Frankel AD (2002): Simulations of Seismic Hazard for the Pacific Northwest of the United States from Earthquakes Associated with the Cascadia Subduction Zone. *Pure and Applied Geophysics,* **159**(9), 2147–2168.

[6] Osteraas J, Krawinkler H (1989): The Mexico Earthquake of September 19, 1985—Behavior of Steel Buildings. *Earthquake Spectra,* **5**(1), 51–88.

[7] Uetani K, Tagawa H (1996): Deformation Concentration Phenomena in the Process of Dynamic Collapse of Weak-Beam-Type Frames. *Journal of Structural and Construction Engineering (Transactions of AIJ),* **61**(483), 51–60.

[8] Uemura S, Uetani K (2018): Overall Plastic Buckling Phenomena and its Suppression Methods part 2 Characteristic analysis of twist collapse phenomenon using simple model. *Summaries of technical papers of Annual Meeting*, 401–402.

[9] Shanley FR (1947): Inelastic Column Theory. *J Aeronaut Sci,* **14**(5), 261–268.

[10] Fukuda I, Ikago K Year, "Global Buckling Analysis of High-Rise Steel Moment-Resisting Frames Involving Inelastic Torsional Deformation Concentration," in *12th Pacific Structural Steel Conference*, Tokyo, Japan.

[11] Hill R (1958): A General Theory of Uniqueness and Stability in Elastic-Plastic Solids. *J Mech Phys Solids,* **6**(3), 236–249.

[12] Hill R (1957): On the Problem of Uniqueness in the Theory of a Rigid-plastic Solid—IV. *J Mech Phys Solids,* **5**(4), 302–307.

[13] Hill R (1957): On the Problem of Uniqueness in the Theory of a Rigid-Plastic Solid—III. *J Mech Phys Solids,* **5**(3), 153–161.

[14] Hill R (1956): On the Problem of Uniqueness in the Theory of a Rigid-plastic Solid—II. *J Mech Phys Solids,* **5**(1), 1–8.

[15] Hill R (1956): On the Problem of Uniqueness in the Theory of a Rigid-plastic Solid—1. *J Mech Phys Solids,* **4**(4), 247–255.

